

An experimental and Finite Element analysis of radii and skew effects on interior permanent magnet motors performance

Ali Jabbari

Department of Mechanical Engineering, Faculty of Engineering,
Arak University,
Arak 38156-8-8849, Iran

Copyright © 2013 ISSR Journals. This is an open access article distributed under the **Creative Commons Attribution License**, which permits unrestricted use, distribution, and reproduction in any medium, provided the original work is properly cited.

ABSTRACT: Effect of rotor iron pole radii and skew on performance of interior permanent magnet motors is studied in this paper. A comparison is carried out by finite element analysis method and is confirmed by the experimental results obtained with two laboratory prototypes. The results show that, although the skew method is very effective in suppressing the cogging torque of an interior permanent magnet (IPM) motor, it will deteriorate other performances more in respect to radii ratio method.

KEYWORDS: Interior permanent magnet motor, pulsating torque minimization, rotor iron pole radii, skew ratio.

1 INTRODUCTION

Recently, interior permanent magnet (IPM) motors have been widely used in electric vehicles, washing machines, air conditioner, etc. because of their high efficiency and easy speed control. However, cogging torque which arises due to the interaction between rotor permanent magnets and slotted stator may cause vibration and acoustic noises.

A broad variety of techniques for minimizing cogging torque is documented in the literature for permanent magnet machines. Among various approaches, skewing is known to be the most effective method for reducing of the cogging torque in permanent magnet (PM) machines [1-8].

Several studies have been conducted to reduce cogging torque using shape optimization. Table I summarizes the literature by showing the type of optimization approach. In [9], the reduction of the cogging torque as well as the improvement of the flux waveform is achieved by suitably shaping the geometry of the polar piece. In [10], the shape of flux barriers is optimized by finite element method to reduce the cogging torque in an interior permanent magnet synchronous motor. The effect of the position of the flux barriers on the torque ripple is analytically studied and experimentally verified by [11]. Using the continuum sensitivity analysis approach coupled by the finite element analysis method, rotor shape optimization is investigated by [12] to reduce cogging torque of an interior permanent magnet motor without deteriorating other performances. Segmented IPM machine is proposed to provide an improved flux-weakening capability and to reduce cogging torque by [13]. The continuum shape design sensitivity formula and the finite element method are employed to calculate the sensitivity of flux-linkage to the design variables, which determine the shape of iron pole piece by [14]. In [15], a rotor pole shape proposed which consists of a uniform and an eccentric surface in order to reduce cogging torque, torque ripple, and harmonics of back EMF waveform in spoke-type brushless DC motor in [16]. An optimal shape design obtained by drilling small circular holes in the rotor is reported by [17]. They stated that an optimal location and radius of the holes effectively reduces the torque pulsation of the IPM motor.

Table 1. Specification of the investigated IPM motor

Researcher	Shaping Case	Cost Function
[1]	polar piece geometry	cogging torque, flux waveform
[2]	flux barriers	cogging torque
[3]	the position of the flux barriers	torque ripple
[4]	rotor shape	cogging torque
[5]	segmented IPM	flux-weakening, cogging torque
[6]	iron pole shape	flux-linkage
[7]	rotor pole shape	cogging torque, torque ripple, back EMF waveform
[8]	circular holes in the rotor	torque pulsation

2 IPM MOTOR DESIGN

In Fig. 1, a cross-section of the investigated motor which is a 3 phases, 8 poles-18 slots is shown and characteristics of the motor are listed in Table II.

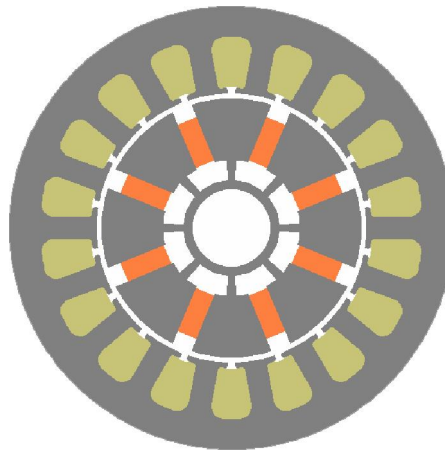


Fig. 1. Cross section of 8P18S IPM motor

Table 2. Specification of the investigated IPM motor

Parameter	Value
Outer Diameter	115 mm
Pole number	8
Slot number	18
Phase number	3
PM flux density	1.17 T

3 RADII RATIO AND SKEW RATIO DEFINITION

Radii ratio is the ratio of rotor iron pole radius to maximum allowable radius of iron pole piece and is represented by ρ , i.e.

$$\rho = \frac{R}{R_{\max}} \quad (1)$$

In this research, the effect of rotor iron pole radii on motor performance has been investigated, by selecting 64 radius in interval of [11, 33.5] mm with a step size of 0.5mm. Therefore, the ρ value is in interval of [0.328, 1].

Skew ratio is defined as the ratio of slot skew angle to slot pitch angle and is represented by α . Peak cogging torque curve versus skew ratio has four local minimum points. The position of these points is consistent with the results of the following equation:

$$\alpha_{sk} = k \frac{N_s}{N_l} \quad (2)$$

Where, $k = 1, 2, \dots, \frac{N_l}{N_s}$. For the investigated motor,

$$\alpha_{sk} = k \frac{18}{18 \times 4} = \frac{k}{4} \quad (k = 1, 2, 3, 4)$$

Therefore the optimal α_{sk} will be 0.25, 0.5, 0.75, and 1. Peak cogging torque shape is sine like. In $\alpha=1$, all harmonics of cogging torque will be cancelled.

4 EFFECT OF RADII RATIO AND SKEW RATIO ON MOTOR PERFORMANCE

In this section, the effect of radii ratio and skew ratio on motor performance has been studied. Motor performance can be classified as

- Peak cogging torque,
- Electromagnetic torque ripple,
- Reluctance torque ripple.
- Peak Back-EMF value,
- V-THD value,
- Efficiency.

Pulsating torque can be calculated with the sum of cogging, electromagnetic and reluctance torque components.

4.1 PEAK COGGING TORQUE VALUE COMPARISON

By reducing the radii ratio (ρ), peak cogging torque value (T-pk) decreases significantly from 0.01827N.m (at $\rho=1$) to 0.0001003N.m (at $\rho=0.343$) and then increases slightly to 0.0001668N.m (at $\rho=0.328$), as shown in Fig. 2. In other words, a parabolic curve with a minimum at $\rho=0.343$ can be adopted for cogging torque variations respect to radii. By reducing the radii, peak cogging torque variation rate decreases gradually from a sharp slope of 70.6° (at $\rho=1$) to 0.126° (at $\rho=0.343$).

By increasing skew ratio from zero to 0.25, peak value of cogging torque decreases with a sharp slope. From skew ratio of 0.25 to 0.375, peak value of cogging torque increases and then decreases to 0.5.

4.2 PEAK BACK-EMF VALUE COMPARISON

By reducing the radii, peak value of Back-EMF reduces from 108.718V (at $\rho=1$) to 107.936V (at $\rho=0.895$) with a constant slope of 7.4° . Continuing the process of reducing the radii, peak value of Back-EMF increases to 119.382V with a constant slope of 16.06° (at $\rho=0.328$). In other words, motor nominal voltage reduces from 217.436V (at $\rho=1$) to 215.874V (at $\rho=0.895$) and then increases to 238.778V (at $\rho=0.328$).

Peak value of Back-EMF decreases from 108.718V (at $\alpha=0$) to 105.566V (at $\alpha=1$), as shown in Fig. 3. This means that motor nominal voltage decreases from 215.436V to 211.132V.

4.3 MOTOR EFFICIENCY COMPARISON

Motor efficiency in respect to radii is drawn in Fig. 4. Motor efficiency decreases gradually from 82.8% (at $\rho=1$) to 79.5% (at $\rho=0.328$). At optimal radii, motor efficiency value is 81.7%.

By increasing skew ratio, motor efficiency decreases from 82.8 % (at $\alpha=0$) to 80.5% (at $\alpha=1$) as shown in Fig. 4.

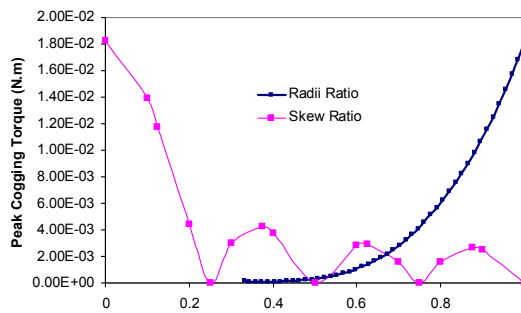


Fig. 2. Peak cogging torque variations respect to rotor iron pole radii

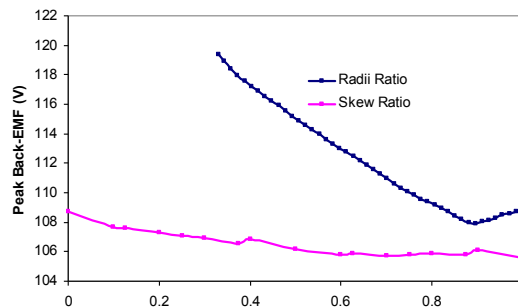


Fig. 3. Peak Back-EMF waveform versus skew ratio

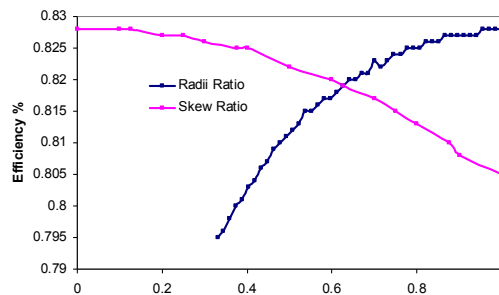


Fig. 4. Motor efficiency versus skew ratio

4.4 ELECTROMAGNETIC TORQUE RIPPLE COMPARISON

As shown in Fig. 5, electromagnetic torque ripple decreases from 0.01139N.m (at $\rho=0.582$) and then increases to 0.0205799N.m (at $\rho=0.328$).

Electromagnetic torque ripple decreases from 0.0761 (at $\alpha=0$) to 0.0125999N.m (at $\alpha=1$).

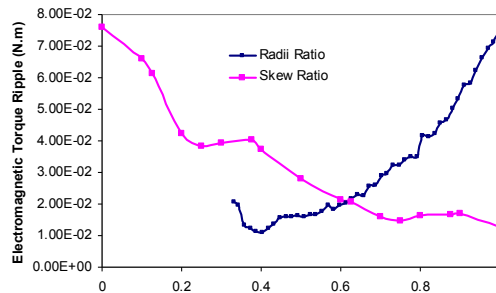


Fig. 5. Electromagnetic torque ripple versus skew ratio

4.5 V-THD COMPARISON

By reducing the radii, THD decreases with a constant slope of 14.57° from 8.44% (at $\rho=1$) to 1.51% (at $\rho=0.582$) and then increases with a constant slope of 19.29° to 6.79% (at $\rho=0.328$).

By increasing skew ratio, V-THD decreases from 8.44% (at $\alpha=0$) to 2.7% (at $\alpha=1$), as shown in Fig. 6.

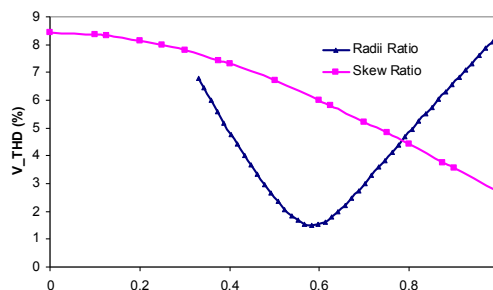


Fig. 6. V-THD versus skew ratio

4.6 RELUCTANCE TORQUE RIPPLE

By reducing the radii, as shown in Fig. 7, average reluctance torque decreased to zero and then increases by further radii reduction, whereas, by increasing skew ratio, average reluctance torque will not decrease considerably.

By reducing the radii, reluctance torque ripple decreases from 0.0170016N.m (at $\rho=1$) to 0.000363207N.m (at $\rho=0.477$) and then increases to 0.0051337N.m (at $\rho=0.328$), as shown in Fig. 8.

By increasing skew ratio, reluctance torque ripple decreases from 0 to 0.25, increases from 0.25 to 0.375, decreases from 0.375 to 0.6, increases from 0.6 to 0.625, decreases from 0.625 to 0.75, increases from 0.75 to 0.875, decreases from 0.875 to 1. By increasing skew ratio, reluctance torque ripple will be decreased. Maximum value is 0.0761 N.m (at $\alpha=0$) and minimal value is 0.0126N.m (at $\alpha=1$), as shown in in Fig. 8.

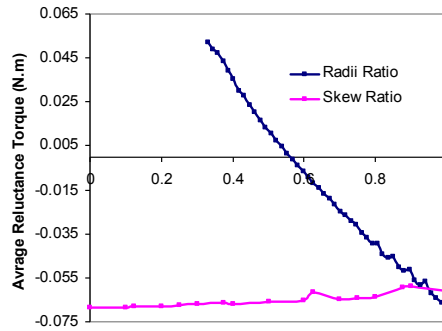


Fig. 7. Reluctance torque versus skew ratio

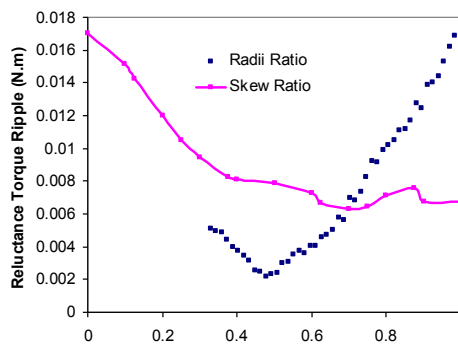


Fig. 8. Reluctance torque versus skew ratio

5 EFFECT OF RADII RATIO AND SKEW ON MOTOR WAVEFORM

In this section, the effect of radii ratio and skew ratio on motor performance components waveforms is compared.

5.1 COGGING TORQUE WAVEFORM COMPARISON

Cogging torque waveforms versus mechanical degree for different radii is drawn in Fig. 9. With a comparison of these curves, it can be found that the number of resting points is constant (9points) from 1 to 0.477 and then increases to 65 (at $\rho=0.343$). In other words, the frequency of cogging torque waveform is constant from 1 to 0.492 and then increases. So the position and the number of peaks and valleys will be changed after 0.492. Therefore, the peak and valley positions in pulsating torque waveform will also be shifted.

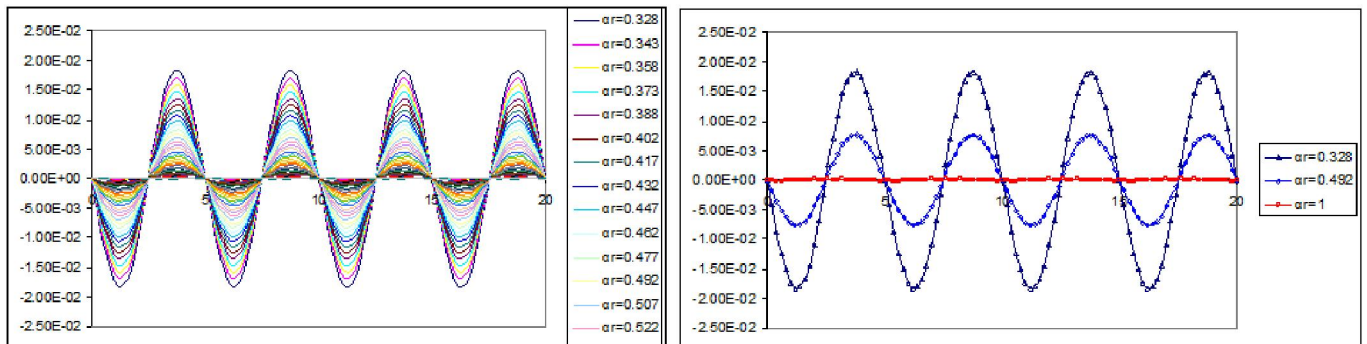


Fig. 9. Cogging torque versus mechanical degree for different radii

As shown in Fig. 10, after each minimal point, the position of peak and valley in the curve shifted by 2° mechanical degree, but the number of resting points is constant.

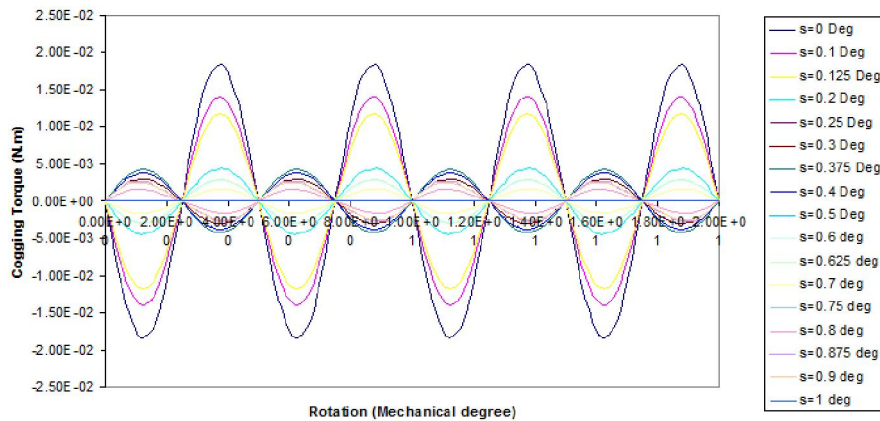


Fig. 10. Cogging torque versus skew ratio

5.2 BACK-EMF WAVEFORM COMPARISON

By reducing the radii, back-EMF waveform closes from a trapezoidal shape (at $\rho=1$) to a sinusoidal one (at $\rho=0.522$) and then diverted from sinusoidal (to $\rho=0.328$) as shown in Fig. 11.

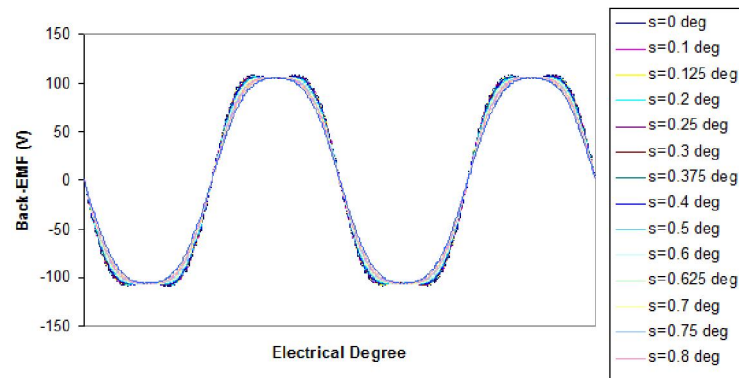


Fig. 11. Back-EMF waveform versus electrical degree for different radii

As shown in Fig. 12, by increasing skew ratio, Back-EMF waveform closes from a trapezoidal shape (at $\alpha=0$) to a sinusoidal one ($\alpha=1$), so that it has the least deviation from sinusoidal shape at $\alpha=1$ (V-THD=2.7%).

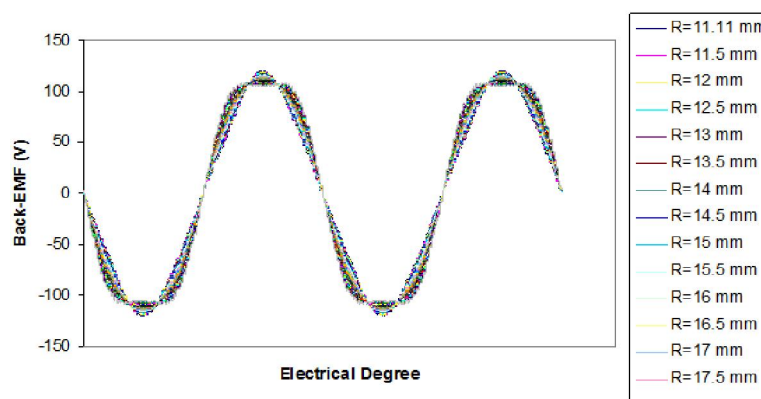


Fig. 12. Back-EMF waveform versus skew ratio

5.3 ELECTROMAGNETIC TORQUE WAVEFORM COMPARISON

As shown in Fig. 13, by increasing skew ratio, higher harmonics of electromagnetic torque will be canceled.

As shown in Fig. 14, frequency of electromagnetic torque fluctuations decreases by reducing the radii. This means that the number of resting points per 180° electrical degree decreases.

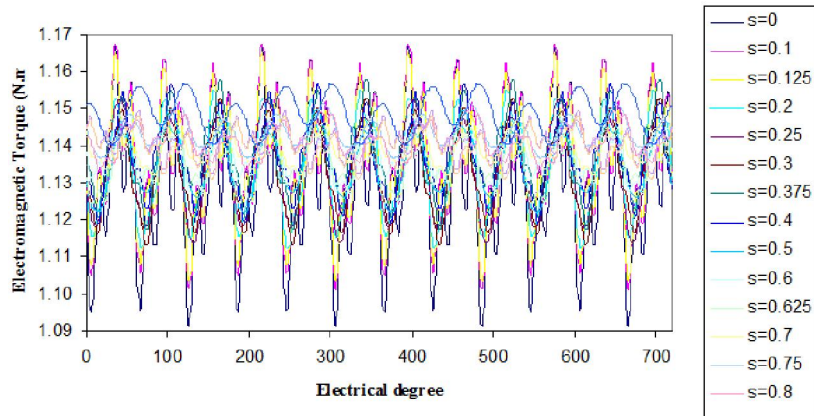


Fig. 13. Electromagnetic torque versus skew ratio

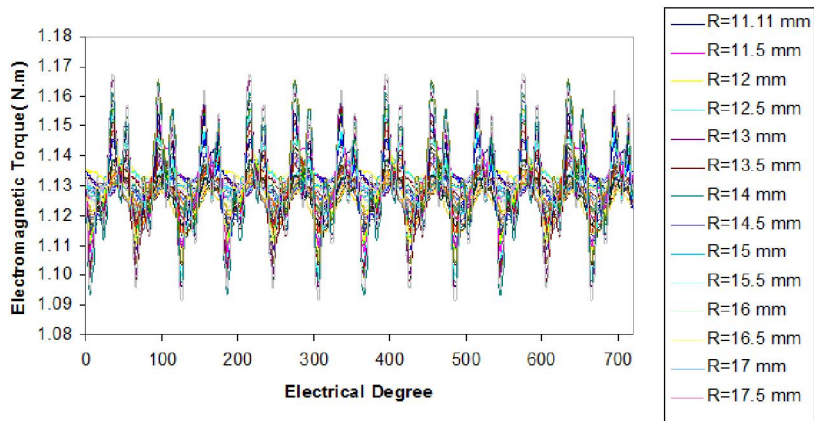


Fig. 14. Electromagnetic torque waveform versus radii

5.4 RELUCTANCE TORQUE WAVEFORM COMPARISON

As shown in Fig. 15, by reducing the radii, average value of reluctance torque reaches from -0.0085008N.m (at $\rho=1$) to zero (at $\rho=0.477$) and then to 0.00256685N.m (at $\rho=0.328$).

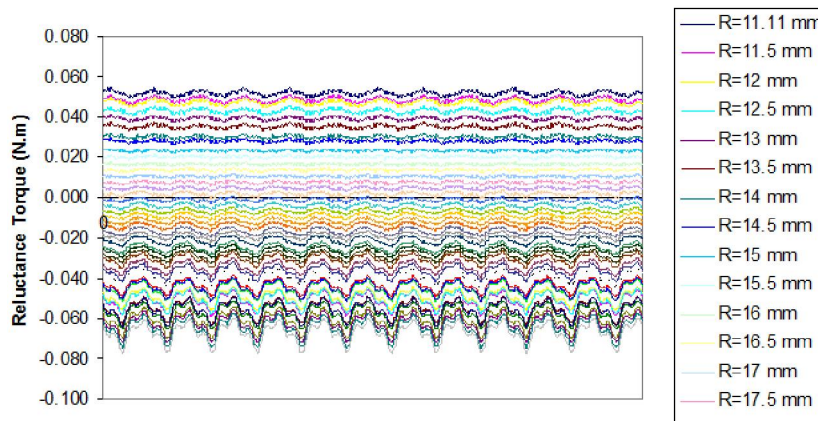


Fig. 15. Reluctance torque waveform versus radii

Reluctance torque waveform is drawn for different skew ratios as shown in Fig. 16. A comparison with the effect of radii, average value of reluctance torque and its frequency does not change considerably. In other words, average value does not close to zero even at $\alpha=1$.

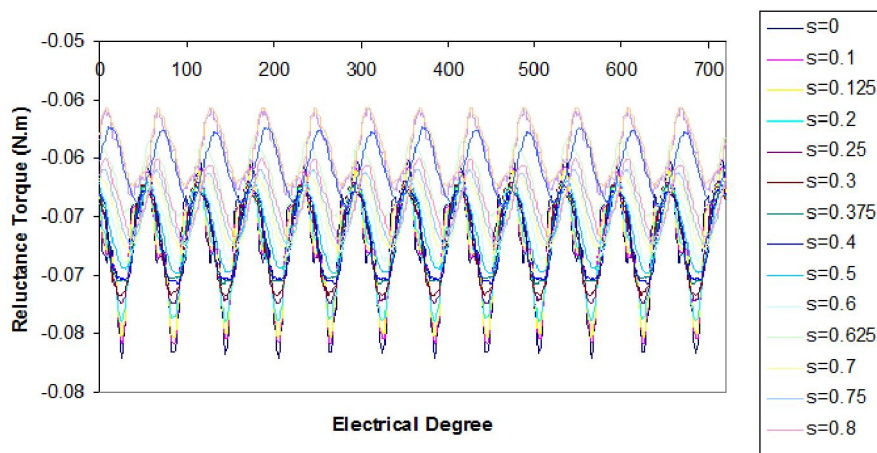


Fig. 16. Reluctance torque versus electrical degree for different skew ratios

6 EXPERIMENTAL RESULTS

The initial and optimal design of the investigated motor is shown in Fig. 17. The experimental results were obtained using the two laboratory prototypes fabricated based on initial and optimal design.

Based on the initial experimental set-up of the Fig. 18, a comparison of Back-EMF for initial and optimal design is shown in Fig. 19. The results show that after optimization of radii, V-THD will be decreased 82% (from 9.12% at $r=33.5\text{mm}$ to 1.64% at $r=19.5\text{ mm}$) which is in good agreement with the FEM analysis result at optimum radii (82.1%).

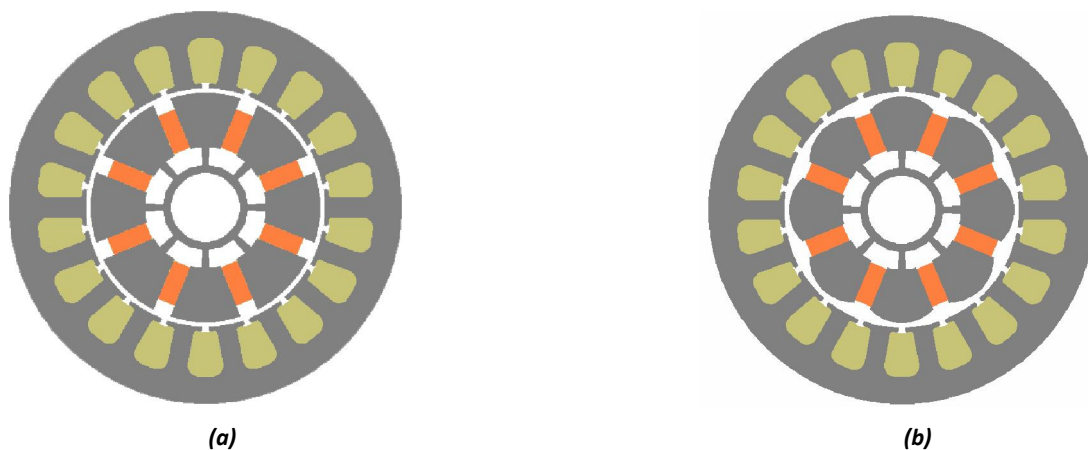


Fig. 17. IPM motor, (a) initial rotor, (b) optimized rotor



Fig. 18. Experimental set-up

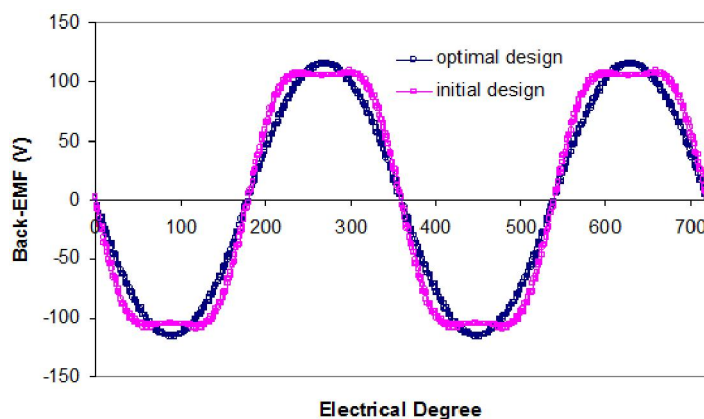


Fig. 19. A comparison of Back-EMF for initial and optimal design

7 CONCLUSION

The effect of radii and skew ratio effect on motor performance is studied first by finite element analysis method and then is validated by experiment. Comparison results show that radii shape optimization is more effective than optimal skew ratios in reducing pulsating torque components.

REFERENCES

- [1] Rajesh P. Deodhar, David A. Staton, Thomas M. Jahns, and J. E. Miller, "Prediction of Cogging Torque Using the Flux-MMF Diagram Technique," *IEEE Transactions on Industry Applications*, vol. 32, no. 3, May/June 1996.
- [2] D.C. Hanselman, "Effect of skew, pole count and slot count on brushless motor radial force, cogging torque and back EMF," *IEE Proc-Electr. Power Appl.*, vol. 144, no. 5, September 1997.
- [3] G.H. Jang, J.W. Yoon, K.C. Ro, N.Y. Park and S.M. Jang, "Performance of a Brushless DC Motor due to the Axial Geometry of the Permanent Magnet," *IEEE Transactions on Magnetics*, vol. 33, no. 5, September 1997.
- [4] M. Łukaniszyn, M. Jagieła, and R. Wróbel, "Optimization of Permanent Magnet Shape for Minimum Cogging Torque Using a Genetic Algorithm," *IEEE Transactions on Magnetics*, vol. 40, no. 2 March 2004.
- [5] Min Dai, Ali Keyhani, and Tomy Sebastian, "Torque Ripple Analysis of a PM Brushless DC Motor Using Finite Element Method," *IEEE Transactions on Energy Conversion*, vol. 19, no. 1, March 2004.
- [6] Mohammad S. Islam, Sayeed Mir, Tomy Sebastian, and Samuel Underwood, "Design Considerations of Sinusoidally Excited Permanent-Magnet Machines for Low-Torque-Ripple Applications," *IEEE Transactions on Industry Applications*, Vol. 41, No. 4, July/August 2005.
- [7] Delvis Anibal González, Juan Antonio Tapia, and Alvaro Letelier Bettancourt, "Design Consideration to Reduce Cogging Torque in Axial Flux Permanent-Magnet Machines," *IEEE Transactions on Magnetics*, vol. 43, no. 8, August 2007.
- [8] Li Zhu, S. Z. Jiang, Z. Q. Zhu, and C. C. Chan, "Analytical Methods for Minimizing Cogging Torque in Permanent-Magnet Machines," *IEEE Transactions on Magnetics*, vol. 45, no. 4, April 2009.
- [9] E.R. Braga Filho and A.M.N. Lima, "Reducing Cogging Torque in Interior Permanent Magnet Machines without Skewing," *IEEE Transactions on Magnetics*, vol 34, no 5, September 1998.
- [10] Y. Kawaguchi, T. Sato, I. Miki, and M. Nakamura, "A Reduction Method of Cogging Torque for IPMSM," 2007 *IEEE*.
- [11] Nicola Bianchi, Silverio Bolognani, Diego Bon, and Michele Dai Pr'e, "Rotor flux-barrier design for torque ripple reduction in synchronous reluctance motors," 2006 *IEEE*.
- [12] Dong-Hun Kim, Il-Han Park, Joon-Ho Lee, and Chang-Eob Kim, "Optimal Shape Design of Iron Core to Reduce Cogging Torque of IPM Motor," *IEEE Transactions on Magnetics*, vol. 39, no. 3, May 2003.
- [13] Rukmi Dutta, Saad Sayeef and M. F. Rahman, "Cogging Torque Analysis of a Segmented Interior Permanent Magnet Machine," 2007 *IEEE*.
- [14] Joon-Ho Lee, Dong-Hun Kim, and Il-Han Park, "Minimization of Higher Back-EMF Harmonics in Permanent Magnet Motor Using Shape Design Sensitivity With B-Spline Parameterization," *IEEE Transactions on Magnetics*, vol. 39, no. 3, May 2003.

- [15] Kyu-Yun Hwang, Sang-Bong Rhee, Byoung-Yull Yang, and Byung-Il Kwon, "Rotor Pole Design in Spoke-Type Brushless DC motor by Response Surface Method," *IEEE Transactions on Magnetics*, vol. 43, no. 4, April 2007.
- [16] A. Kioumars, M. Moallem, and B. Fahimi, "Mitigation of Torque Ripple in Interior Permanent Magnet Motors by Optimal Shape Design," *IEEE Transactions on Magnetics*, vol. 42, no. 11, November 2006.
- [17] Sung-Il Kim, Ji-Young Lee, Young-Kyoun Kim, Jung-Pyo Hong, Yoon Hur, and Yeon-Hwan Jung, "Optimization for Reduction of Torque Ripple In Interior Permanent Magnet By Using the Taguchi Method," *IEEE Transactions on Magnetics*, vol. 41, no. 5, 2005.